ChemPubSoc Europe

DOI: 10.1002/chem.201403164

CHEMISTRY
A European Journal
Full Paper

Hybrid Helices

New Helical Folds in α-Peptides with Alternating Chirality

Gangavaram V. M. Sharma,*[a] Gajulapati Venkateshwarlu,[a] Pothula Purushotham Reddy,[b] and Ajit C. Kunwar*[b]

Abstract: In α-peptides, the 8/10 helix is theoretically predicted to be energetically unstable and has not been experimentally observed so far. Based on our earlier studies on 'helical induction' and 'hybrid helices', we have adopted the 'end-capping' strategy to induce the 8/10 helix in α-peptides by using short α/β-peptides. Thus, α-peptides containing a regular string of α-amino acids with alternating chirality were end capped by α/β-peptides with 11/9-helical motifs at the termini. Extensive NMR spectroscopy studies of these peptides revealed the presence of a hitherto unknown 8/10-helical pattern; the H-bonds in the shorter pseudorings were rather weak. The approach of using short helical motifs to induce new mixed helices in α-peptides could provide avenues for more versatile design strategies.

Introduction

Peptides and proteins fold into complex three-dimensional structures, through fundamental elements such as helices, strands, and turns, for performing their functions. De novo designs have been extensively investigated for the past two decades in order to mimic peptide and protein structures and their diverse functions, in addition to addressing their limitations for executing novel functions.[1] Such an effort in 1996 led to the first reports on the unusually robust 14-helical patterns in short β-peptides.[2] The molecules, which take well-defined predictable structures, were referred to as 'foldamers'.[3] Subsequent studies led to diverse folding patterns with novel structures and functions, including a unique 12/10 mixed helix,[4] which, unlike the other secondary structures, has a periodicity at the dimer level that leads to H-bonded pseudorings of different sizes.[5] The mixed helix exhibited distinctive intertwined H-bonds (N–H^{i+1}···O–C^{i+2} and N–H^{i+2}···O–C^{i-1}, termed as $i \rightarrow (i+1)/i \leftarrow (i+3)$ interactions). After the first reports on regular α/β-peptides[6] with heterogeneous backbones and the discovery of an 11/9 helix,[7] several other mixed helices,[8] such as the 11/13 and 12/14 helices in α/γ-, β/γ-, α/δ-, and α/ε-peptides, that follow a similar H-bonding arrangement were identified. More recently, Martinek, Reiser, and co-workers[9] found 16/18 mixed helices in α/β-peptides, which contained expanded H-bonded pseudorings and were stabilized by $i \rightarrow (i+3)/i \leftarrow (i+5)$ interactions.

Historically, gramicidin A,[10] derived from alternating D- and L-α-amino acids, displayed the first mixed helix, which was referred to as the β helix. This helix was a 20/22 mixed helix, with 20- and 22-membered intertwined H-bonds (N–H^{i+1}···O–C^{i+6} and N–H^{i+6}···O–C^{i-1}, respectively) involving $i \rightarrow (i+5)/i \leftarrow (i+7)$ interactions and having 6.3 residues per turn. Yet another mixed helix with $i \rightarrow (i+3)/i \leftarrow (i+5)$ interactions, the 14/16 mixed helix (with 4.4 residues per turn), which often appeared in equilibrium with a double-helical species, was reported in α-peptides derived from norleucine residues with alternating chirality.[11] A 14/16 helix was also reported by Zweier and co-workers[12] in oligomers of Gly in the gaseous phase.

Ab initio calculations by Hofmann and co-workers[13] suggested that the periodic helices are energetically favored in homologous α-, γ-, and δ-peptides, relative to the mixed helices in polar media. However, for α-peptides, larger H-bonding pseudorings, like those in a 14/16 helix, with $i \rightarrow (i+3)/i \leftarrow (i+5)$ interactions, are the preferred option in apolar media.[13,14] Hofmann and co-workers[13] have found theoretically that an 8/10 helix in α-peptides is not viable in the gaseous phase. However, in peptides from δ-amino acids, which are isosteres of α-dipeptides, 8- and 10-membered H-bonding has been shown to be energetically favorable.

Gellman and co-workers observed the induction of an α-helix in a small octameric α-peptide in chimeric (α/β+α) peptides[15] by a short α/β-peptide[7a] at the N terminus. A similar concept of 'hybrid helices'[16] was elaborated by our group; compatibility was found among different types of mixed helices. In a similar effort, by using this concept, we were able to induce helicity in β-HGly oligomers[17] by end capping with short 12/10-helical β-peptides[4,18] or with a single chiral β-Caa (a C-linked carbo-β-amino acid) residue. Furthermore, in a new design with α/β-peptides with alternating α,α,β,β-peptide re-

[a] Dr. G. V. M. Sharma, G. Venkateshwarlu+
Organic and Biomolecular Chemistry Division
CSIR—Indian Institute of Chemical Technology, Hyderabad 500 007 (India)
E-mail: esmvee@iict.res.in

[b] P. P. Reddy,+ Dr. A. C. Kunwar
Centre for Nuclear Magnetic Resonance and Structural Chemistry
CSIR—Indian Institute of Chemical Technology, Hyderabad 500 007 (India)
E-mail: kunwar@iict.res.in

[+] These authors contributed equally to this work.

Supporting information for this article (NMR, IR, and CD spectra, details of the MD calculations, and experimental details for compounds **1–3**) is available on the WWW under http://dx.doi.org/10.1002/chem.201403164.

peats, Martinek, Reiser, and coworkers[9] identified the presence of an interesting 9/12/10/9-helical pattern. This design depicts the presence of two α residues in between β residues or two β residues adjacent to two α residues.

Inspired by the above findings,[15–17] we designed peptides by end capping short oligomers of α residues (with alternating chirality) with α/β-peptides (11/9 helix)[7a] for inducing helicity, in the anticipation of achieving the elusive 8/10-helical fold.[13] The enhancement of helical stability with such end capping in α-peptides by appropriate α-amino acids at the N terminus is well established.[19] Thus, as a first step, it was proposed to tether a small oligomeric sequence of Ala (L-Ala–D-Ala–L-Ala and L-Ala–D-Ala–L-Ala–D-Ala–L-Ala) to a small 11/9-helical fragment of an α/β-peptide (alternating β-Caa and L-Ala) at the N terminus and at both the N and C termini. In the present communication, we report the results of the synthesis of peptides **1**, **2**, and **3** (Figure 1) and their folding propensities, as determined by NMR spectroscopy, CD spectroscopy, and molecular dynamics studies.

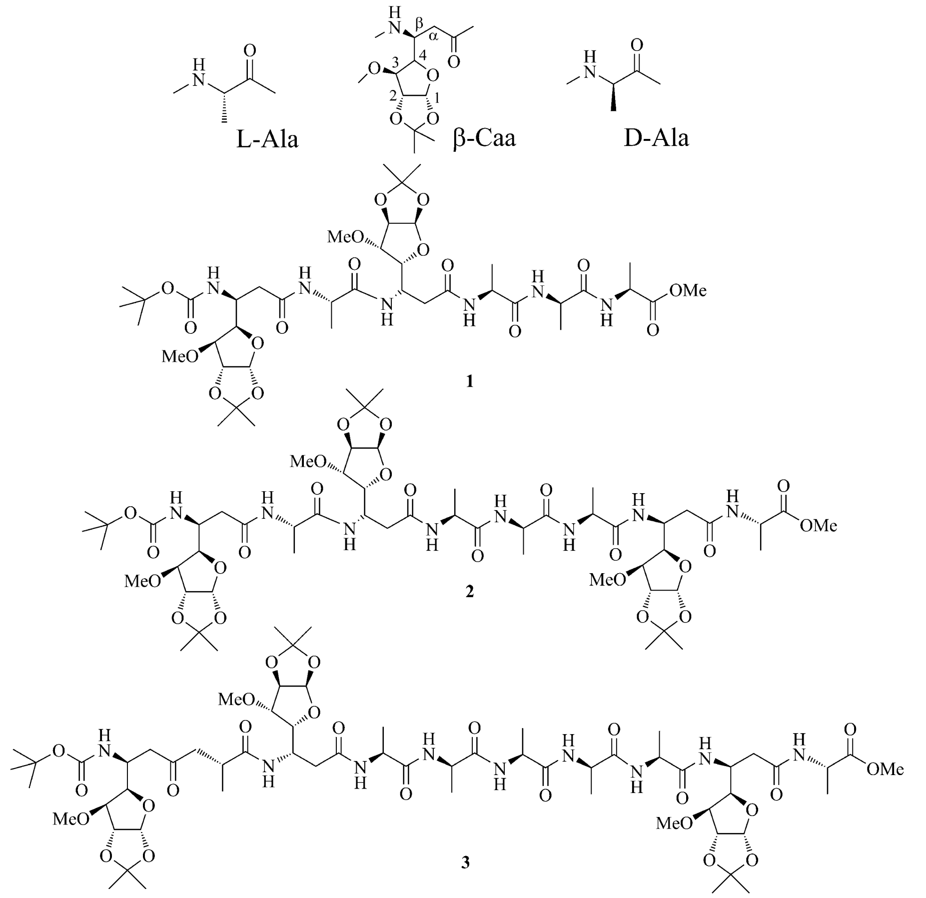

Figure 1. Structures of peptides **1**–**3**.

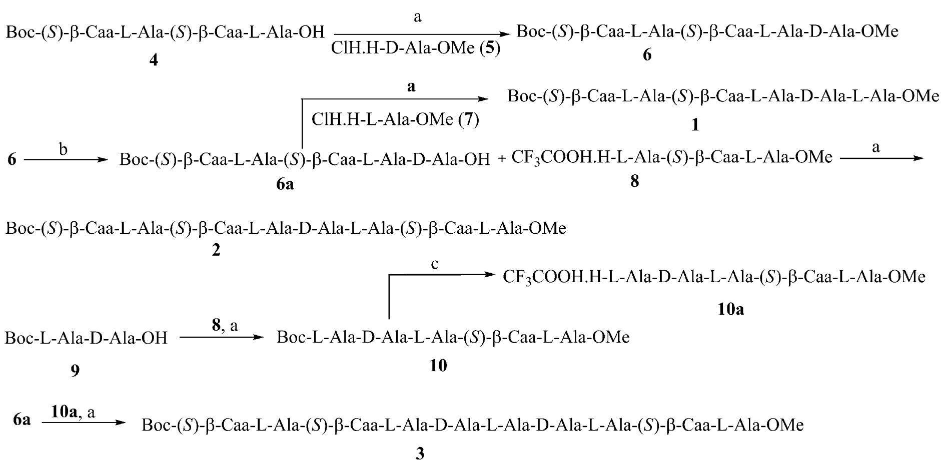

Scheme 1. Synthesis of peptides **1**–**3**: a) HOBt, EDCI, DIPEA, dry CH_2Cl_2, 0 °C→RT; b) LiOH, THF:MeOH:H_2O (3:1:1), 0 °C→RT; c) CF_3COOH, dry CH_2Cl_2, 2 h.

Results and Discussion

Peptide synthesis

Peptides **1**, **2**, and **3** (Figure 1; residue numbers in our subsequent discussions have been marked with an italic superscript) were synthesized under standard peptide coupling conditions[20] by using 3-(3-dimethylaminopropyl)-1-ethylcarbodiimide (EDCI), 1-hydroxy-1*H*-benzotriazole (HOBt), and *N*,*N*-diisopropylethylamine (DIPEA) in the solution phase.[21]

The known tetrapeptide acid[7a] **4** upon coupling with salt **5** (Scheme 1), prepared from D-Ala, gave pentapeptide **6** in 65% yield. Base (LiOH) hydrolysis of peptide **6** at 0 °C to room temperature afforded pentapeptide acid **6a** (89%), which upon coupling with salt **7**, prepared from L-Ala, furnished hexapeptide **1** (58%).

Likewise, acid **6a** upon coupling with known salt **8**[7a] gave octapeptide **2** in 42% yield. Similarly, acid **9** upon coupling with **8** afforded pentapeptide **10** (62%), which furnished the corresponding salt **10a** after exposure to CF_3COOH in CH_2Cl_2 for two hours. Furthermore, acid **6a** upon coupling with salt **10a**, in the presence of EDCI, HOBt, and DIPEA in CH_2Cl_2 at room temperature for 5 h, furnished decapeptide **3** (34%).

Conformation analysis

NMR studies on peptides **1**–**3** were undertaken in $CDCl_3$ and CD_3OH in approximately 5 mM solutions (at temperatures of 233–313 K).[21] In peptide **1**, the Ala sequence at the C terminus is tethered with β-Caa–L-Ala–β-Caa, which has a high propensity to form an 11/9 helix,[7a] stabilized by $NH^{i+1}\cdots CO^{i+2}$ and $NH^{i+2}\cdots CO^{i-1}$ H-bonds. In the ^{1}H NMR spectrum ($CDCl_3$, 288 K) of **1**, four of the amide protons have chemical shifts (δNH) greater than 7 ppm, which indicates their likely participation in H-bonding. Solvent titration studies[22] show that, except for NH^2 and NH^5, the other amide protons have rather modest variation in their chemical shift values ($\Delta\delta NH < 0.72$ ppm), which confirms their involvement in H-bonding. At 248 K, the $^3J_{NH-C\beta H}$ (8.0, 8.5 Hz) and $^3J_{C\alpha H-C\beta H}$ (4.1–6.0 Hz) values for the β-Caa residues and the $^3J_{NH-C\alpha H}$ values (5.0, 5.5 Hz) for L-Ala^2 and L-Ala^4 justify C(O)–N–Cβ–Cα (φ_β), N(H)–Cβ–Cα–C(O) (θ_β), and C(O)–N–Cα–C(O) (φ_α) for an 11/9 helix.[7a,13,21,23] D-Ala^5 displayed a $^3J_{NH-C\alpha H}$ value of 8.6 Hz, which implies $\varphi_\alpha \approx 120^\circ$. Excluding the terminal residues, the strong sequential nuclear Overhauser effect (NOE) correlations of $C\alpha H^i/NH^{i+1}$ [$i=2$–4; for β-Caa^3, it is CαH(pro-*R*)^3/NH^4] fixed N–Cα–C(O)–N (ψ_α) as approximately 120° for L-Ala^2, and L-Ala^4 and Cβ–Cα–C(O)–N (ψ_β) as approximately −120° for β-Caa^3. For the D-Ala^5 NOE correlations, NH^5/NH^6 and NH^6/CαH^4 support $\psi_\alpha \approx -60^\circ$. The NOE correlations (Figure 2) NH^3/NH^4, NH^5/NH^6, NH^1/CβH^3, NH^4/CαH^2, NH^3/CαH^5, NH^6/CαH^4, C4H^1/CαH(pro-*R*)^3, C3H^1/NH^4, C4H^1/NH^4, C3H^3/NH^6, and C4H^3/NH^6 and the above inferences provide the distinctive signature of an 11/9 helix at the N terminus and the propagation of a similar H-bonding pattern along the length of **1**. This extension of a mixed helix at the C terminus is further supported by the $^3J_{NH-C\alpha H}$ values of 8.6 and 6.5 Hz for the last two residues, which leads to an alternation of large and small amide proton ^3J values throughout the length of the peptide. Additionally, despite the fraying in the termini, the involvement of NH^6 in H-bonding also sustains the above deductions.

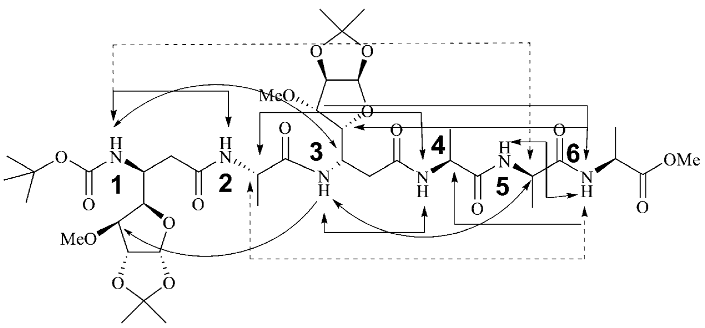

Figure 2. Characteristic NOE correlations for model helices h_1 (solid line) and h_2 (dotted line).

The IR studies of **1** in chloroform solution additionally provided adequate support for the participation of several amide protons in H-bonding. Two sets of bands were observed in the amide stretch region,[21] in which the one at 3424 cm^{-1} with lower intensity is attributed to the amides that are not H-bonded, whereas the other one at 3318 cm^{-1} with strong intensity corresponds to the H-bonded amide protons.

In spite of the presence of the structural fold discussed above, the NOE correlations NH^1/CαH^5 and NH^6/CαH^2 imply the intriguing presence of yet other structure. Such distinctive NOE correlations were noticed by Navarro et al.[11] for 14/16 helices. Thus, to understand the presence of two families of helices, we followed the approach adopted by Gellman and co-workers[6a] in their pioneering work on the 'split personality' involving rapid interconversion between 11 and 14/15 helices in regular α/β-peptides. Thus, two model helices, one with a $i\rightarrow(i+1)/i\leftarrow(i+3)$ interaction (model helix h_1) and the other, model helix h_2, with a $i\rightarrow(i+3)/i\leftarrow(i+5)$ interaction, were generated (Figure 3). In the absence of adequate information about such helices, as a first step, we generated helix h_1 with the dihedral angles deduced from the ^3J values and NOE correlations and minimized the structure by imposing the required H-bond constraints and constraining the dihedral angle ω (Cα–C(O)–N–Cα for α-amino acids and Cα–C(O)–N–Cβ for β-Caa) to (180±20)°, in order to sustain *trans*-amide bonds. For model helix h_2, the φ_β, θ_β, ψ_β, φ_α, and ψ_α values were taken from the data of Hofmann and co-workers[13] and Navarro et al.[11] for the first four and last two residues, respectively, and then the structure was minimized by imposing the above-mentioned constraints on the dihedral angle ω and the expected H-bonding constraints, which display a 16/18 helix at the N terminus and a 14/16 helix at the C terminus. In addition to the H-bonds, the model helix h_2 confirms the distinguishing NOE correlations of NH^1/CαH^5 and NH^6/CαH^2 (Table 1). The defining signatures of such hybrid helices are shown in Table 1. To obtain the distances from the ROESY spectra in $CDCl_3$, an isolated spin approximation was used.[25] The backbone dihedral angles in h_1 and h_2 are very similar, so the interconversion between them is facile, as was also the case reported for $3_{10}\rightarrow$

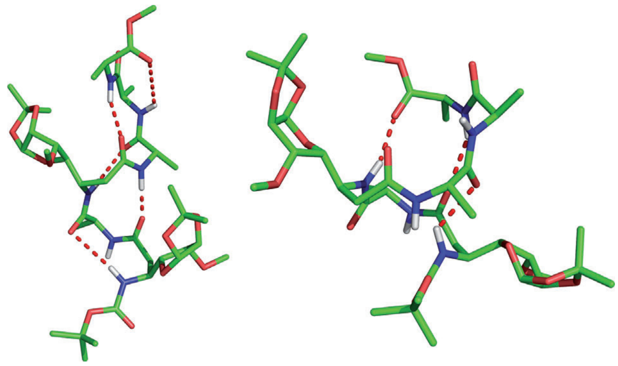

Figure 3. Structures of model helices A) h_1 and B) h_2 for **1**.

Table 1. Internuclear distances in peptide **1** for the model helices h_1 and h_2 and those derived from the ROESY spectra in $CDCl_3$ at 248 K (A)[25] and the NOE intensities in CD_3OH at 233 K (B).

	h_1 [Å]	A [Å]	B[a]	h_2 [Å]		h_1 [Å]	A [Å]	B[a]	h_2 [Å]
NH^{1}/NH^{2}	2.6	4.3	m	4.1	CαH^{2}/NH^{4}	3.2	3.4	m	3.9
NH^{1}/CβH^{3}	4.7	4.5	–[b]	4.8	CαH^{2}/CαH^{5}	5.8	–[c]	–[b]	6.0
NH^{1}/CαH(pro-*R*)^{3}	4.2	5.0	w	3.2	CαH^{2}/NH^{6}	6.7	4.0	–[b]	2.2
NH^{1}/NH^{4}	4.5	–[c]	w	2.5	NH^{3}/NH^{4}	2.5	3.9	m	4.2
NH^{1}/CαH^{5}	9.3	4.4	–[c]	2.4	NH^{3}/CαH^{5}	4.4	3.1	w	5.7
C3H^{1}/NH^{4}	4.1	3.9	m	6.8	C3H^{3}/NH^{6}	3.2	4.0	m	7.5
C4H^{1}/CαH(pro-*R*)^{3}	3.4	3.7	m	6.0	C4H^{3}/NH^{6}	3.1	3.8	m	5.5
C4H^{1}/NH^{4}	3.4	–[b]	–[b]	4.9	C4H^{3}/CαH^{5}	3.5	4.2	m	6.8
C4H^{1}/CαH^{5}	8.7	–[c]	–[c]	3.8	CαH^{4}/NH^{6}	4.0	3.4	m	5.8
C4H^{1}/NH^{6}	8.3	–[c]	–[c]	3.6	NH^{5}/NH^{6}	2.5	3.3	m	3.9

[a] NOE intensities have been qualitatively described as strong (s), medium (m), or weak (w), for which the upper limits for the distances are 2.5, 3.5, and 5.0 Å, respectively. [b] Overlapping NOE correlations. [c] NOE correlations were not observed.

α-helix (in proteins)[24] and 11→14/15helix interconversions in α/β-peptides.[6a]

Figure 4 shows expansions of the ROESY spectra of **1** at various temperatures. The dominance of the h_1 helix population over that of h_2 was evident upon lowering of the temperature from 288 to 248 K, because the NOE correlations NH^{4}/CαH^{2} and NH^{6}/CαH^{4} became stronger relative to NH^{6}/CαH^{2}. Similarly, changes in the ^{3}J values with temperature, especially those in the $^{3}J_{NH-C\alpha H}$ value for L-Ala, also support the above observations.[21] Thus, due to the presence of two helical folds, even at the lowest temperatures, it was decided not to carry out the molecular dynamics (MD) calculations, because the NOE cross peaks in the ROESY data would contain information that would be averaged over both of them.

Having observed the presence of two helices in **1** in $CDCl_3$, a detailed study was undertaken in methanol at 288 and 233 K.[21] The intramolecular H-bonding in CD_3OH was probed by recording spectra at different temperatures between 288 and 253 K and determining the temperature coefficients of the amide proton chemical shifts ($\Delta\delta/\Delta T$). The $|\Delta\delta/\Delta T| >$ 9.0 ppb K^{-1} values for NH^{1}, NH^{3}, and NH^{5} imply that they are solvent exposed, whereas the $|\Delta\delta/\Delta T| < 2.0$ ppb K^{-1} values for the other residues (all L-Ala, except L-Ala^{2}) reveal that they are solvent shielded, because of their involvement in H-bonds. Very similar alternation of the $\Delta\delta/\Delta T$ values were observed by Martinek, Reiser, and co-workers[9] in their studies on 16/18-helically folded α/β-peptides. They interpreted the data as supporting helical structures with H-bonds right through the length of the peptides. Further confirmation for the involvement of amide protons in H-bonding was inferred from the ^{1}H–^{2}H exchange studies in CD_3OD as a function of time. Although the resonances for NH^{5} and NH^{6} disappeared after approximately 2 and 4 h, respectively, others persisted even after 12 h, which supported strongly their participation in H-bonding.[21]

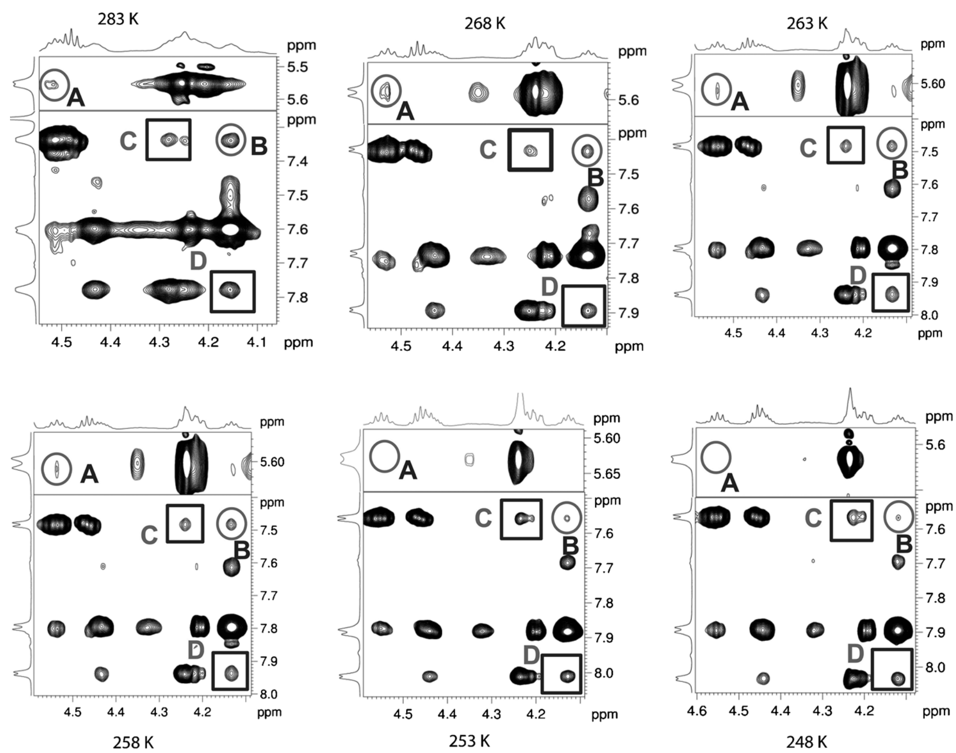

Figure 4. Expansions of the ROESY spectra of peptide **1** in $CDCl_3$ at various temperatures. The NOE correlations A(NH^{1}/CαH^{5}) and B(CαH^{2}/NH^{6}) (circled) characterize the h_2 helix, whereas C(CαH^{4}/NH^{6}) and D(CαH^{2}/NH^{4}) (inside the squares) are distinctive for the h_1 helix.

At 233 K, for β-Caa residues, $^{3}J_{NH-C\beta H} = 9.7$ and 8.1 Hz and $^{3}J_{C\alpha H-C\beta H} = 3.8$ Hz (β-Caa^{3}); for the L-Ala residues, $^{3}J_{NH-C\alpha H} = 2.2$–4.3 Hz. These values are consistent with an 11/9 helix.[7a] For the middle residues (β-Caa and L-Ala), values of $\psi_\alpha \approx 120°$ and $\psi_\beta \approx -120°$ are adequately supported by the strong sequential NOE correlations, CαH^{i}/NH^{i+1} [$i =$ 2–4; for β-Caa^{3}, NH^{4}/CαH(pro-*R*)^{3}]. For D-Ala^{5}, $^{3}J_{NH-C\alpha H} = 7.7$ Hz, which infers a preponderance of $\varphi_\alpha \approx 120°$. As discussed earlier for D-Ala^{5}, the NOE correlations NH^{5}/NH^{6} and NH^{6}/CαH^{4} imply $\psi_\alpha \approx -60°$. The amide proton couplings again alternate between small and large values. Thus, the above deductions and the distinctive NOE correlations of NH^{1}/NH^{2}, NH^{3}/NH^{4}, NH^{4}/CαH^{2}, NH^{6}/CαH^{4}, NH^{1}/CβH^{3}, and NH^{3}/CαH^{5} support the helix h_1. The lack of distinctive signatures of the h_2 model suggests their near absence for **1** in methanol solution.[21]

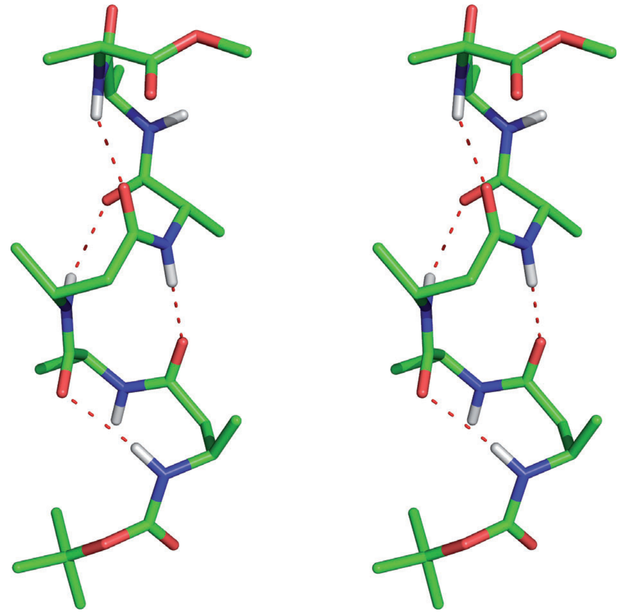

Figure 5. Stereoview of the minimum energy structure from the MD calculations of peptide **1**. Hydrogen atoms and side chains have been removed for clarity after the calculations.

This provided us with the impetus to undertake MD studies on **1**. The structure refinement of peptide **1** by MD calculations was carried out by using the experimental NMR restraints, the distance and dihedral angle constraints.[21] The distance constraints were deduced from the qualitative data from the ROESY spectra, whereas the dihedral angle constraints, as deduced above from the couplings and NOE correlations, were used for the residues in the middle excluding the ones in the two termini. However, in view of the large $^3J_{NH-C\beta H}$ value for β-Caa^1, the φ_β value was constrained. The MD calculations were initiated with the geometry of the model helix h_1. Figure 5 shows a stereoview of the lowest energy structure obtained from the MD studies. The H-bond defining distances between the (N)H and O(C) groups ($r_{(N)H-O}$) for the NH^4···CO^1, NH^6···CO^3, NH^1···CO^2, and NH^3···CO^4 H-bonds are, respectively, 2.09, 2.15, 2.37, and 2.58 Å, which very clearly demonstrate the presence of the 11/9 helix at the N terminus and the nucleation of the 8/10 helices. However, the structure does not reflect the proximity of NH^5 and CO^6, probably due to a lack of sufficient constraints involving the terminal residues, which results in fraying.

The CD spectrum of peptide **1** in methanol shows a maxima at about 202 nm and a weak shoulder at approximately 225 nm.[21] These characteristics are disctinctive signatures of an 11/9 helix.[7a] We believe this supports a continued presence of an $i \rightarrow (i+1)/i \leftarrow (i+3)$ interaction through the length of the peptide.

The ^{1}H spectrum of octapeptide **2**, end capped at both the termini with an 11/9 helix, at 278 K in $CDCl_3$ shows several amide resonances with δNH > 7 ppm, which suggests the participation of these protons in H-bonding. Solvent titration studies[22] showed that, except for the first two residues, all of the other amide protons display $\Delta\delta$NH < 0.59 ppm and are predominantly H-bonded. Emphatic support for such intramoleculary H-bonded amide protons is found from the IR data, in which two bands were observed in the amide stretch region, at 3423 cm^{-1} (lower intensity band arising from non-H-bonded amide) and 3317 cm^{-1} (strong intensity band corresponding to the H-bonded amides).

The $^3J_{NH-C\beta H}$ couplings for the β residues were greater than 8.0 Hz and the $^3J_{NH-C\alpha H}$ values for the L-α residues were less than 6.0 Hz (except for the last residue, which has a value of 7.8 Hz). In fact, D-Ala^5 has $^3J_{NH-C\alpha H}$ = 9.0 Hz and, thus, alternation of the amide couplings like that in peptide **1** is also noticed here. For β-Caa^3 and β-Caa^7, strong NOE correlations, CαH$_{(pro-S)}$^{3}/C3H^3 and CαH$_{(pro-S)}$^{7}/C3H^7, allowed the stereospecific assignments of the Cα protons. The above information, along with NOE correlations involving the side chains, C4H^1/CαH$_{(pro-R)}$^{3}, C3H^1/NH^4, C4H^1/NH^4, C3H^3/NH^6, and C4H^3/NH^6, enabled us to restrict φ_α to approximately −60° for the L-Ala residues (except for L-Ala^8). For D-Ala^5, $^3J_{NH-C\alpha H}$ = 7.5 Hz, which supports a φ_α value of around 120°. Furthermore, for the first, third, and seventh β-Caa residues, the $^3J_{NH-C\beta H}$ values of 8.0, 8.5, and 9.5 Hz, respectively, are also consistent with values of approximately 120° for φ_β. Like the hexamer, the presence of strong sequential NOE correlations, NH^i/CαH^{i-1} (i = 2–7; for the β-Caa^3 and β-Caa^7, the NOE correlations NH^4/CαH(pro-S)^3 and NH^8/CαH(pro-S)^7 are involved), indicates $\psi_\alpha \approx 120°$, $\psi_\beta \approx -120°$, and $\psi_\alpha \approx -60°$. (For D-Ala^5, the presence of NH^5/NH^6 and NH^6/CαH^4 justifies this.) The presence of several NH^i/NH^{i+1} correlations (i = 1, 5, and 7) and the alternation of the amide proton couplings support mixed-helix folding. The two hybrid helix models h_1 and h_2[21] were constructed for **2**, as for **1**. The model helix h_1 was derived from the dihedral angles deduced from the ^3J values and the NOE correlations with imposition of the required H-bonding and ω constraints. Similarly, for the h_2 model helix, the values reported by Hofmann and co-workers[13] were used for the residues at the termini, whereas the values given by Navarro et al.[11] were used for the residues in the middle. Subsequently, the structure was minimized by imposing the desired H-bonding and ω constraints.[21]

The support for the h_1 model helix appears to be overwhelming with the prominent presence of NOE correlations NH^1/CβH^3, CαH^2/NH^4, CαH^4/NH^6, and CαH^6/NH^8 (Figure 6), especially at lower temperatures in CH_2Cl_2 solution.[21] The characteristic NOE correlations, NH^1/CαH^5 and CαH^2/NH^6, for the h_2 model helix were also observed. Careful studies undertaken to find the variation in couplings with temperature also supported the above observations.[21] Noticeable among them was the reduction in the $^3J_{NH-C\alpha H}$ value for the L-α-amino acid residues with lowered temperatures. Due to spectral broadening, such variations in couplings were not as distinct as those observed in methanol solution. In view of the presence of two types of folds in rapid exchange in the $CDCl_3$ solution, the MD calculations were yet again not undertaken, because the constraints derived from the couplings and the ROESY data would reflect contributions from both the families of foldings.

The ^{1}H NMR spectra of **2** in CD_3OH were studied as a function of temperature in the range 298–253 K. The $\Delta\delta/\Delta T$ values yet again alternated between small and large values and showed

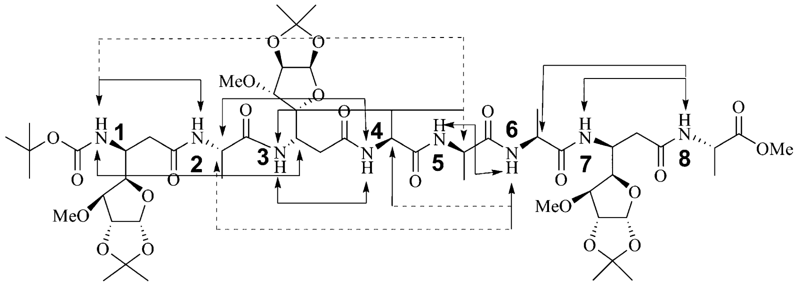

Figure 6. Characteristic NOE correlations for model helices h_1 (solid line) and h_2 (dotted line) for peptide **2**.

bonded pseudorings display longer and, thus, weaker H-bonds. This may well be a reflection of the protic nature of the solvent (methanol), in which the stability of the helices is compromised due to their participation in H-bonding with the solute.

In the ^{1}H NMR spectrum (CDCl$_3$, 278 K) of **3**,[21] except for

a similar trend to that observed for **1**. The amide protons of the β-Caa and D-Ala residues display $|\Delta\delta/\Delta T| > 8.0$ ppb K^{-1}, whereas $|\Delta\delta/\Delta T| < 5.3$ ppb K^{-1} for L-Ala residues (except L-Ala^2). Thus, a helical structure was deduced, in analogy with the reported results from Martinek, Reiser and co-workers.[9] Interestingly, the ^{1}H–^{2}H exchange studies showed that all of the amide proton resonances are present even after 5 h and 5 amide resonances persisted beyond 14 h, which further strongly supports an underlying H-bonded structure.

Detailed studies for **2** in CD$_3$OH were carried out at 263 K. For the β-Caa^1, β-Caa^3, and β-Caa^7 residues, the $^3J_{\text{NH-C}\beta\text{H}}$ values are 9.0, 8.3, and 8.5 Hz, respectively, which support $\varphi_\beta \approx 120°$. For the L-Ala residues, $^3J_{\text{NH-C}\alpha\text{H}} = 3.8$, 2.6, 4.0, and 6.5 Hz (second, fourth, sixth, and eighth residues, respectively) and these values, along with NOE correlations involving the side chains C4H^1/CαH(pro-*R*)^3, C3H^1/NH^4, C4H^1/NH^4, C3H^3/NH^6, and C4H^3/NH^6, are consistent with $\varphi_\alpha \approx -60°$. The $^3J_{\text{NH-C}\alpha\text{H}}$ value of 8.2 Hz for the D-Ala^5 is consistent with $\varphi_\alpha \approx 120°$, which demonstrates a regular alternation of large and small couplings involving the amide protons through the length of **2**, a requirement for the continued 11/9-helix-like folding in the middle of the peptide, as per model helix h_1. In addition, the strong sequential NH^i/CαH^{i-1} ($i = 2$–7) correlation supported values of $\psi_\alpha \approx 120°$ and $\psi_\beta \approx -120°$. Small values of $^3J_{\text{C}\alpha\text{H-C}\beta\text{H}}$ (3.4 and 6.5 Hz for the first residue, 4.1 and 5.9 Hz for the third residue, and 4.8 and 5.1 Hz for the seventh residue) are consistent with $\theta_\beta \approx 60°$. The NOE correlations NH^1/NH^2, NH^5/NH^6, NH^7/NH^8, NH^1/CβH^3, CαH^2/NH^4, NH^3/CαH^5, CαH^4/NH^6, and CαH^6/NH^8, as well as the above deductions on dihedral angles, provide unmistakably the distinctive signatures of an 11/9 helix at the N and C termini, in addition to the continuation of a helix with a similar H-bonding pattern in the middle, in agreement with the model helix h_1. The results emphatically support the propagation of such a fold in the core, consisting of α-amino acids, of the peptide.

The spectra in CD$_3$OH showed the signatures of only the model helix h_1, so MD calculations were undertaken for **2**. Figure 7 shows a stereoview of the lowest energy structure obtained from the MD studies. The induction of 8/10-helical folds is distinctly noticeable, although in the shorter H-bonded pseudorings, especially the 8-mer, the NH^5 and CO^6 electrostatic interaction is rather weak, with $r_{\text{(N)H-O}} = 3.63$ Å, whereas the $r_{\text{(N)H-O}}$ values for the NH^4···CO^1, NH^6···CO^3, NH^8···CO^5, NH^1···CO^2, and NH^3···CO^4 interactions are respectively 2.02, 2.12, 2.00, 2.89, and 2.70 Å. The data appear to show that the shorter H-

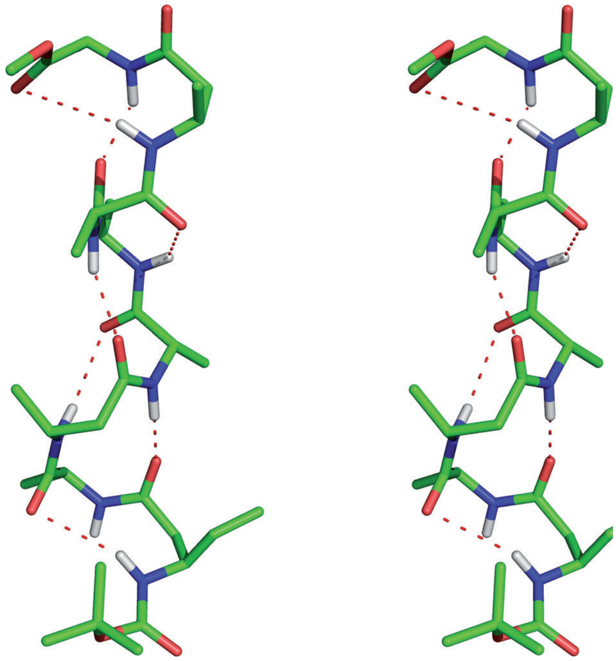

Figure 7. Stereoview of the minimum energy structure from the MD calculations of peptide **2**. Hydrogen atoms and side chains have been removed for clarity after the calculations.

the first two residues and D-Ala^7, all of the other amide protons are H-bonded (δNH > 7.43 ppm and ΔδNH < 0.51 ppm).[22] Also, δNH = 5.65 ppm and ΔδNH = 0.77 ppm for β-Caa^1 and δNH = 7.43 ppm and ΔδNH = 0.69 ppm for D-Ala^7, which suggests a preponderance of their involvement in H-bonds. Yet again, the IR data strongly support the participation of most of the amide protons in intramolecular H-bonds.[21] In the IR spectrum, two bands were observed, at 3422 cm^{-1} and 3318 cm^{-1}, with lower intensity (from non-H-bonded amides) and stronger intensity (from H-bonded amides), respectively. Unlike in **1** and **2**, the $^3J_{\text{NH-C}\beta\text{H}}$ values for β-Caa (6.7–8.4 Hz) and the $^3J_{\text{NH-C}\alpha\text{H}}$ values for Ala residues (4.0–6.8 Hz) do not follow the alternation pattern.[21] For β-Caa residues, the $^3J_{\text{NH-C}\beta\text{H}}$ and $^3J_{\text{C}\alpha\text{H-C}\beta\text{H}}$ values (4.3–6.0 Hz) justify φ_β and θ_β for a right-handed 11/9 helix at the termini.[7a,13,23] As discussed above, the model helices h_1 [$i\rightarrow(i+1)/i\leftarrow(i+3)$ interaction with 9/11- and 8/10-helical folds] and h_2 [$i\rightarrow(i+3)/i\leftarrow(i+5)$ interaction with 16/18- and 14/16-helical folds] were generated.[21]

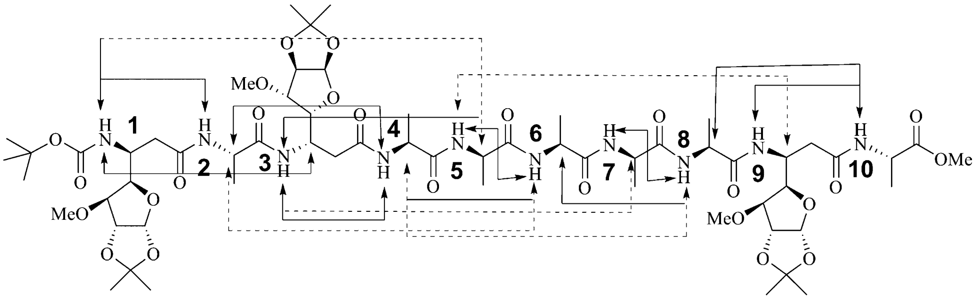

Figure 8. Characteristic NOE correlations for model helices h_1 (solid line) and h_2 (dotted line) for peptide **3**.

The ROESY spectrum shows NOE correlations for NH^i/CαH^{i+4} (i=1, 3, and 5) and CαH^i/NH^{i+4} (i=2 and 4; Figure 8), which strongly support a high propensity of the h_2 helical fold through the length of the peptide. On the other hand, the NOE correlations of NH^i/NH^{i+1} (i=1, 5, 6, and 9), C4H^1/CαH-(pro-*R*)^3, C3H^1/NH^4, C4H^1/NH^4, C3H^3/NH^6, and C4H^3/NH^6 suggest the persistence of an 11/9 helix at the termini, whereas the continuity of such a helix is compromised in the core of the oligomer. The studies in methanol, however, provided more convincing evidence for the structure. These results are further supported by the CD spectrum of peptide **2** in methanol, in which a maxima at about 202 nm and a weak shoulder at approximately 225 nm are very similar to those in the 11/9 helix.[7a,21]

For **3**, the variable-temperature studies in CD_3OH (258–298 K) show that all β-Caa and D-Ala residues have $|\Delta\delta/\Delta T| >$ 7.0 ppb K^{-1}, which indicates their exposure to the solvent. However, for the L-Ala residues, $|\Delta\delta/\Delta T| <$ 6.0 ppb K^{-1} (except L-Ala^2), which suggests the participation of these residues in intermolecular H-bonding. From the model helix h_1, this information implies that the participation of the amide protons in H-bonding with shorter pseudorings (8- and 9-mer) is weak. ^{1}H–^{2}H exchange studies of **3** in CD_3OD further showed that 8 of the amide resonances survived even after 4 h, which corroborates their involvement in H-bonding. However, the NH^5 and NH^7 resonances lasted for approximately 1 h, which confirmed the results from the variable-temperature studies. At 253 K, for β-Caa residues, $^3J_{NH-C\beta H}$ (8.4–9.6 Hz), $^3J_{C\alpha H-C\beta H}$ (3.5–7.4 Hz), and for L-Ala residues (2.8–6.7 Hz) are consistent with an 11/9 helix at the termini. The values for D-Ala residues (8.1 and 7.4 Hz) support $\varphi_\alpha \approx 120°$. In the ROESY spectrum, the NH^i/NH^{i+1} (i=1, 3, 5, 7, and 9) and CαH^i/NH^{i+2} (i=2, 4, 6, and 8) NOE correlations emphatically justify the h_1 model helix for **3**. Unlike in the shorter peptides, the signatures of model helix h_2 are not present for **3**.

MD calculations were performed as discussed for the other peptides. A stereoview of the minimum energy structures for **3** obtained from the MD calculations is shown in Figure 9. Yet again, like the other peptides, the data appear to suggest that, in CD_3OH, the NH···CO distances for the shorter pseudorings are rather large, which suggests weaker H-bonds. The $r_{(N)H-O}$ values for NH^4···CO^1, NH^6···CO^3, NH^8···CO^5, NH^{10}···CO^7, NH^1···CO^2, NH^3···CO^4, NH^5···CO^6, and NH^7···CO^8 interactions are 2.01, 2.19, 2.31, 2.09, 2.57, 2.87, 3.29, and 3.49 Å, respectively. At the C terminus, due to insufficient constraint, the expected NH^9···CO^{10} H-bond does not appear, although we occasionally observed structures with NH^9 in the proximity of the oxygen atom of the terminal methoxy group. For the minimum energy structure, this distance was 2.56 Å. The CD spectrum of peptide **3** in methanol supports these findings of the presence of an $i\rightarrow(i+1)/i\leftarrow(i+3)$ interaction throughout the length of the oligomer.[7a,21] By using the φ_α and ψ_α values from the middle residues (residues 5–7) for D-Ala as 131° and −56°, respectively, and the corresponding values of −70° and 116° for the L-Ala residues, the deduced 8/10 helix is characterized by a pitch of approximately 7.5 Å with about 4 residues per turn.

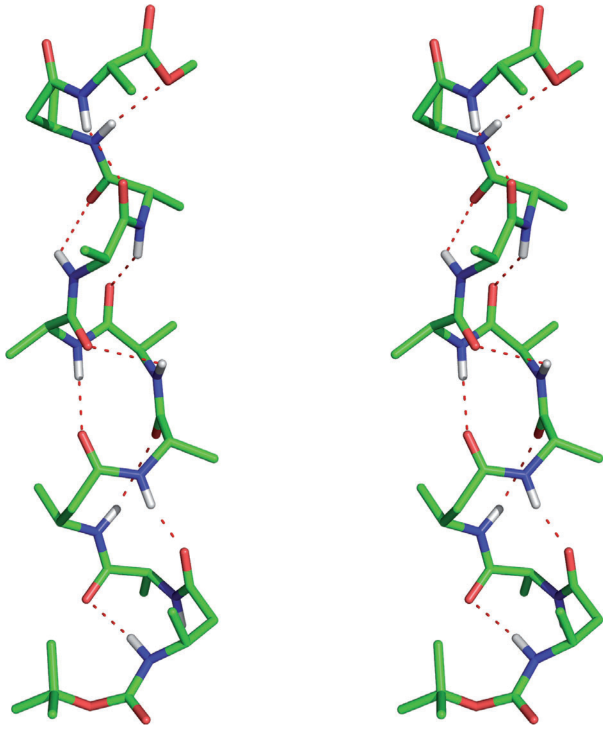

Figure 9. Stereoview of the minimum energy structure from the MD calculations of peptide **3**. Hydrogen atoms and side chains have been removed for clarity after the calculations.

Conclusion

In the present study, the propagation of an H-bonding pattern throughout the length of an α-peptide with alternating chirality has been demonstrated by using the 'hybrid-helix' approach. The strategy of end capping with α/β-peptides (11/9 helix) at the termini resulted in two interconverting helices in $CDCl_3$, with the predominance of helices with $i\rightarrow(i+1)/i\leftarrow(i+3)$ interactions. On the other hand, in methanol, the string of α-amino acids displayed exclusive nucleation of an 8/10 helix by the 11/9 mixed helix at the termini. However, the helices observed had weaker H-bonds for the shorter psuedorings. This study, thus, acquires importance in paving way for the design of novel α-peptides to create diverse motifs. It is believed that the addition of helix-stabilizing influences may enhance the propensity and stability of these uncommon folding patterns in oligomers of α-amino acids.

Experimental Section

General

NMR spectra (1D and 2D experiments) for peptides **1**–**3**, **6**, and **10** were obtained at 300, 400, 500, and 600 MHz (^{1}H) and at 75, 100, 125, 150, and 175 MHz (^{13}C). Chemical shifts (δ) are reported with respect to internal tetramethylsilane (TMS) as the reference. Information on hydrogen bonding in $CDCl_3$ was obtained from solvent titration studies by sequentially adding of [D$_6$]DMSO (up to 300 μL) into $CDCl_3$ solutions of the peptides (600 μL). Such information in methanol was deduced from variable-temperature experiments and ^{1}H–^{2}H exchange studies. The coupling constants were measured with resolution-enhanced ^{1}H spectra. The States-TPPI procedure was used to run various 2D NMR experiments in the phase-sensitive mode by using standard programs in the library provided by the instrument manufacturer. ROESY experiments were performed with mixing times of 0.2 and 0.3 s by using a continuous spin-locking field of about 2.5 KHz. TOCSY experiments were performed with a spin-locking field of about 10 KHz and a mixing time of 0.08 s. The spectra were acquired with 2×256 or 2×192 free induction decays containing 8–32 transients. The 2D data were processed with Gaussian apodization in both dimensions. IR spectra were recorded with an FTIR spectrometer by using KBr pellets for peptides **6** and **10**; for peptides **1**–**3**, the studies were carried out in $CHCl_3$ solution in the range ν = 400–4000 cm^{-1}. The CD spectra were obtained in 0.2 mM solution in methanol. The values are expressed in terms of the total molar ellipticity (θ) [deg cm^2 dmol^{-1}]. Restraint molecular dynamics studies were carried out by using simulated annealing protocols with the help of the INSIGHT-II Discover module.[21] The MD simulations were carried out on the ROESY data obtained in CD_3OH by using the volume integrals qualitatively. The molecules were subjected to a 2 ns simulated annealing protocol and the lowest energy structures are presented herein.

Boc-(*S*)-β-Caa-L-Ala-(*S*)-β-Caa-L-Ala-D-Ala-OMe (6)

A solution of acid **4** (0.18 g, 0.24 mmol), HOBt (0.04 g, 0.28 mmol), and EDCI (0.05 g, 0.28 mmol) in CH_2Cl_2 (5 mL) was stirred at 0 °C under an N_2 atmosphere for 15 min, treated sequentially with salt **5** [prepared from D-Ala (0.03 g, 0.24 mmol) and concd HCl (cat.) in MeOH (3 mL)] and DIPEA (0.04 mL, 0.36 mmol), and stirred for 8 h. The reaction mixture was quenched with aq saturated NH_4Cl solution (20 mL). After 10 min, it was diluted with $CHCl_3$ (3×10 mL) and washed with water (20 mL), $NaHCO_3$ solution (20 mL), and brine (20 mL). The organic layers were dried (Na_2SO_4) and evaporated and the residue was purified by column chromatography (60–120 mesh silica gel, 1.2% MeOH in $CHCl_3$) to afford **6** (0.13 g, 65%) as a white solid. M.p. 196–198 °C; $[\alpha]_D^{20}$ = 98.73 (c = 0.1 in $CHCl_3$); IR ($CHCl_3$): ν = 3276, 2980, 2925, 2852, 2352, 1711, 1635, 1533, 1453, 1370, 1297, 1247, 1215, 1165, 1117, 1080, 1018, 888, 854, 754, 665, 640 cm^{-1}; ^{1}H NMR ($CDCl_3$, 600 MHz): δ = 7.89 (d, 1 H, J = 7.1 Hz, NH-4), 7.54 (d, 1 H, J = 8.4 Hz, NH-3), 7.14 (d, 1 H, J = 7.5 Hz, NH-5), 6.45 (d, 1 H, J = 3.0 Hz, NH-2), 5.91 (d, 1 H, J = 3.9 Hz, C_1H-1), 5.88 (d, 1 H, J = 3.7 Hz, C_1H-3), 5.60 (d, 1 H, J = 7.6 Hz, NH-1), 4.58 (d, 1 H, J = 3.7 Hz, C_2H-3), 4.57 (d, 1 H, J = 3.9 Hz, C_2H-1), 4.50 (q, 1 H, J = 7.5 Hz, C_αH-5), 4.50 (q, 1 H, J = 7.1 Hz, C_αH-4), 4.43 (ddt, 1 H, J = 8.4, 9.2, 5.0 Hz, C_βH-3), 4.29 (dd, 1 H, J = 2.4, 9.2 Hz, C_4H-3), 4.24 (m, 1 H, C_4H-1), 4.18 (m, 1 H, C_βH-4), 4.05 (dq, 1 H, J = 3.3, 7.2 Hz, C_αH-2), 4.02 (d, 1 H, J = 2.4 Hz, C_3H-3), 3.77 (m, 1 H, C_3H-1), 3.75 (s, 3 H, COOMe), 3.39 (s, 3 H, OMe), 3.36 (s, 3 H, OMe), 2.67 (dd, 1 H, J = 5.0, 13.5 Hz, CαH$_{(pro\text{-}R)}$-3), 2.55 (dd, 1 H, J = 5.0, 14.5 Hz, CαH$_{(pro\text{-}R)}$-1), 2.39 (dd, 1 H, J = 6.0, 14.5 Hz, CαH$_{(pro\text{-}S)}$-1), 2.24 (dd, 1 H, J = 6.0, 14.5 Hz, CαH$_{(pro\text{-}S)}$-3), 1.49 (s, 9 H, Boc), 1.48 (s, 3 H, Me), 1.37 (s, 3 H, Me), 1.30 (s, 3 H, 2×Me), 1.39 (d, 1 H, J = 7.5 Hz, Me-5), 1.38 (d, 1 H, J = 7.1 Hz, Me-4), 1.37 ppm (d, 1 H, J = 7.2 Hz, Me-2); ^{13}C NMR ($CDCl_3$, 150 MHz): δ = 174.21, 172.54, 172.45, 171.25, 171.08, 111.56, 111.49, 105.00, 104.78, 83.92, 83.59, 81.37, 81.29, 80.29, 79.86, 77.56, 57.44, 57.37, 52.64, 50.56, 48.60, 47.86, 46.97, 38.83, 38.37, 28.42, 26.82, 26.67, 26.29, 26.21, 17.17, 16.97, 15.61 ppm; HRMS (ESI+): m/z calcd for $C_{37}H_{62}N_5O_{16}$ [M^+ + Na]: 832.4164; found: 832.4186.

Boc-(*S*)-β-Caa-L-Ala-(*S*)-β-Caa-L-Ala-D-Ala-L-Ala-OMe (1)

A solution of pentapeptide **6** (0.13 g, 0.16 mmol) in THF/MeOH/H_2O (5 mL; 3:1:1) was treated with LiOH (0.06 g, 0.23 mmol) at 0 °C to room temperature. After 1 h, the pH value was adjusted to 2–3 with aq 1 N HCl solution at 0 °C and the mixture was extracted with EtOAc (2×10 mL). The organic layer was dried (Na_2SO_4) and evaporated to give **6a** (0.1 g, 82%) as a white solid, which was used for next reaction without further purification.

A solution of acid **6a** (0.1 g, 0.12 mmol), HOBt (0.02 g, 0.15 mmol), and EDCI (0.29 g, 0.15 mmol) in CH_2Cl_2 (4 mL) was stirred at 0 °C under an N_2 atmosphere for 15 min, treated sequentially with salt **7** [prepared from L-Ala (0.02 g, 0.12 mmol) and concd HCl in MeOH (3 mL)] and DIPEA (0.03 mL, 0.19 mmol), and stirred for 8 h. Workup as described for **6** and purification of the residue by column chromatography (60–120 mesh silica gel, 1.9% CH_3OH in $CHCl_3$) afforded **1** (0.05 g, 58%) as a white solid. M.p. 202–204 °C; $[\alpha]_D^{20}$ = −106.66 (c = 0.1 in $CHCl_3$); IR ($CHCl_3$): ν = 3424, 3318, 3020, 2938, 2833, 1738, 1668, 1520, 1454, 1377, 1297, 1254, 1163, 1119, 1081, 1021, 887, 856, 776 cm^{-1}; ^{1}H NMR ($CDCl_3$, 600 MHz): δ = 8.03 (d, 1 H, J = 5.7 Hz, NH-4), 7.89 (d, 1 H, J = 8.8 Hz, NH-3), 7.56 (d, 1 H, J = 6.3 Hz, NH-6), 7.33 (d, 1 H, J = 8.3 Hz, NH-5), 6.82 (d, 1 H, J = 4.8 Hz, NH-2), 5.95 (d, 1 H, J = 3.7 Hz, C_1H-1), 5.90 (d, 1 H, J = 3.7 Hz, C_1H-2), 5.63 (d, 1 H, J = 8.3 Hz, NH-1), 4.62 (d, 1 H, J = 3.7 Hz, C_2H-1), 4.61 (d, 1 H, J = 3.7, C_2H-2), 4.55 (d, 1 H, J = 6.9 Hz, C_αH-6), 4.45 (dq, 1 H, J = 8.3, 7.2 Hz, C_αH-5), 4.44 (dd, 1 H, J = 8.8, 9.5 Hz, C_βH-3), 4.24 (m, 1 H, C_βH-4), 4.22 (qd, 1 H, J = 7.3, 5.7 Hz, C_α-4), 4.19 (dd, 1 H, J = 2.6, 9.5 Hz, C_4H-3), 4.12 (dq, 1 H, J = 5.0, 7.3 Hz, C_αH-2), 3.89 (d, 1 H, J = 2.6 Hz, C_3H-3), 3.76 (s, 3 H, COOMe), 3.74 (d, 1 H, J = 5.0 Hz, C_3H-1), 3.38 (s, 3 H, OMe), 3.37 (s, 3 H, OMe), 2.67 (dd, 1 H, J = 4.9, 13.5 Hz, C_αH-3), 2.55 (dd, 1 H, J = 4.1, 14.5 Hz, CαH$_{(pro\text{-}R)}$-1), 2.44 (dd, 1 H, J = 6.0, 14.5 Hz, CαH$_{(pro\text{-}S)}$-1), 2.20 (dd, 1 H, J = 13.5, 4.2 Hz, CαH$_{(pro\text{-}S)}$-2), 1.49 (s, 3 H, Me), 1.50 (d, 3 H, J = 7.4 Hz, Me-6), 1.48 (s, 3 H, Me), 1.47 (s, 3 H, Me), 1.44 (s, 3 H, Me), 1.43 (s, 9 H, Boc), 1.40 (d, 3 H, J = 7.2 Hz, Me-5), 1.39 (d, 3 H, J = 7.3 Hz, Me-4), 1.39 (d, 3 H, J = 7.3 Hz, Me-2), 1.32 (s, 3 H, Me), 1.31 (s, 3 H, Me), 1.29 ppm (s, 3 H, Me); ^{1}H NMR (CD_3OH, 600 MHz): δ = 9.65 (d, 1 H, J = 8.0 Hz, NH-3), 9.23 (d, 1 H, J = 7.5 Hz, NH-5), 8.65 (d, 1 H, J = 3.3 Hz, NH-2), 8.36 (d, 1 H, J = 2.2 Hz, NH-4), 7.97 (d, 1 H, J = 4.4 Hz, NH-6), 7.1 (d, 1 H, J = 9.7 Hz, NH-1), 5.83 (d, 1 H, J = 3.9 Hz, C_1H-3), 5.81 (d, 1 H, J = 3.9 Hz, C_1H-1), 4.72 (d, 1 H, J = 3.8 Hz, C_2H-3), 4.72 (d, 1 H, J = 3.72 Hz, C_2H-1), 4.28 (dq, 1 H, J = 7.5, 7.2 Hz, C_αH-5), 4.23 (dq, 1 H, J = 4.4, 7.2 Hz, C_αH-6), 4.23 (dd, 1 H, J = 3.1, 11.2 Hz, C_4H-1), 4.20 (dddd, 1 H, J = 9.7, 11.2, 8.3, 3.7 Hz, C_βH-1), 4.19 (dd, 1 H, J = 3.0, 9.7 Hz, C_4H-3), 4.18 (ddt, 1 H, J = 8.0, 9.7, 3.8 Hz, C_βH-3), 4.12 (dq, 1 H, J = 3.3, 7.2 Hz,

C_{α}H-2), 4.06 (dq, 1 H, J=2.2, 7.2 Hz, C_{α}H-4), 3.87 (dd, 1 H, J=8.3, 14.5 Hz, $C\alpha H_{(pro\text{-}S)}$-1), 3.75 (d, 1 H, J=3.0 Hz, C_3H-3), 3.74 (d, 1 H, J=3.1 Hz, C_3H-1), 3.70 (s, 3 H, COOMe), 3.39 (s, 3 H, OMe), 3.38 (s, 3 H, OMe), 2.68 (dd, 1 H, J=3.8, 13.4 Hz, $C\alpha H_{(pro\text{-}S)}$-3), 2.40 (dd, 1 H, J=3.7, 14.5 Hz, $C\alpha H_{(pro\text{-}R)}$-1), 2.30 (dd, 1 H, J=8.3, 14.5 Hz, $C\alpha H_{(pro\text{-}S)}$-1), 2.03 (dd, 1 H, J=3.8, 13.4 Hz, $C\alpha H_{(pro\text{-}R)}$-3), 1.53 (d, 1 H, J=7.2 Hz, C_3H-6), 1.41 (br, 9 H, Boc and 6 H, 2×Me), 1.35 (d, 1 H, J=7.2 Hz, C_3H-2), 1.35 (d, 1 H, J=7.2 Hz, C_3H-5), 1.33 (d, 1 H, J=7.2 Hz, C_3H-4), 1.28 (s, 3 H, Me), 1.26 ppm (s, 3 H, Me); ^{13}C NMR (CD_3OD, 150 MHz): δ=175.77, 175.10, 174.72, 174.67, 172.77, 172.62, 157.65, 112.81, 112.55, 106.12, 105.96, 84.90, 84.67, 82.45, 82.38, 82.18, 80.64, 80.03, 57.55, 52.66, 51.79, 51.48, 49.98, 49.86, 47.89, 38.59, 38.50, 28.69, 26.91, 26.37, 26.28, 17.72, 17.33, 17.29, 17.16 ppm; HRMS (ESI+): m/z calcd for $C_{40}H_{66}N_6O_{17}$ [M^++Na]: 925.4356; found: 925.4376.

Boc-(*S*)-β-Caa-L-Ala-(*S*)-β-Caa-L-Ala-D-Ala-L-Ala-(*S*)-β-Caa-L-Ala-OMe (2)

A solution of ester **6** (0.26 g, 0.30 mmol) treated as described above gave **6a** (0.23 g, 90%) as a white solid, which was used for the next reaction without further purification.

A solution of **6a** (0.10 g, 0.12 mmol), HOBt (0.01 g, 0.14 mmol), and EDCI (0.22 g, 0.14 mmol) in dry CH_2Cl_2 (5 mL) was stirred at 0 °C for 15 min and treated with the known salt **8**[6a] (0.06 g, 0.11 mmol) and DIPEA (0.03 mL, 0.17 mmol) under a nitrogen atmosphere for 5 h. Workup as described for **6** and purification of the residue by column chromatography (60–120 mesh silica gel, 4.2% MeOH in $CHCl_3$) afforded **2** (0.06 g, 42%) as a white solid. M.p. 230–232 °C; $[\alpha]_D^{20}$=−41.08 (c=0.1 in $CHCl_3$); IR ($CHCl_3$): ν=3423, 3317, 3020, 2996, 2937, 2833, 1727, 1659, 1532, 1455, 1378, 1314, 1297, 1250, 1163, 1119, 1081, 1024, 887, 856, 752 cm^{-1}; ^{1}H NMR ($CDCl_3$, 600 MHz): δ=8.09 (d, 1 H, J=7.8 Hz, NH-8), 7.93 (d, 1 H, J=8.5 Hz, NH-3), 7.86 (d, 1 H, J=4.0 Hz, NH-6), 7.82 (d, 1 H, J=6 Hz, NH-4), 7.66 (d, 1 H, J=9.0 Hz, NH-5), 7.54 (d, 1 H, J=9.5 Hz, NH-7), 6.75 (d, 1 H, J=4.5 Hz, NH-2), 5.92 (d, 1 H, J=3.6 Hz, C_1H-1), 5.88 (d, 1 H, J=3.6 Hz, C_1H-6), 5.88 (d, 1 H, J=3.6 Hz, C_1H-3), 5.52 (d, 1 H, J=8.0 Hz, NH-1), 4.8 (d, 1 H, J=3.6 Hz, C_2H-1), 4.60 (d, 1 H, J=3.6 Hz, C_2H-7), 4.58 (d, 1 H, J=3.6 Hz, C_2H-3), 4.54 (qd, 1 H, J=7.6, 7.8 Hz, C_{α}H-8), 4.48 (dd, 1 H, J=8.5, 5.6 Hz, C_{β}H-3), 4.47 (qd, 1 H, J=7.6, 9.0 Hz, C_{α}H-5), 4.44 (tdd, 1 H, J=9.5, 4.9, 3.5 Hz, C_{β}H-7), 4.34 (qd, 1 H, J=7.5, 4.7 Hz, C_{α}H-7), 4.27 (dd, J=7.0, 3.2 Hz, C_4H-1), 4.23 (qd, 1 H, J=7.0, 6.0 Hz, C_{α}H-4), 4.19 (dd, 1 H, J=9.6, 3.2 Hz, C_4H-7), 4.08 (dd, 1 H, J=9.6, 3.1 Hz, C_4H-3), 4.05 (d, 1 H, J=3.2 Hz, C_3H-7), 4.0 (qd, 1 H, J=7.5, 4.0 Hz, C_{α}H-6), 3.83 (d, 1 H, J=3.1 Hz, C_3H-3), 3.74 (d, J=3.2 Hz, C_3H-1), 3.71 (s, 3 H, COOMe), 3.41 (s, 3 H, OMe), 3.38 (s, 6 H, 2×OMe), 2.97 (dd, J=12.8, 4.9 Hz, $C\alpha H_{(pro\text{-}R)}$-1), 2.64 (dd, 1 H, J=13.3, 4.9 Hz, $C\alpha H_{(pro\text{-}R)}$-7), 2.62 (dd, 1 H, J=12.8, 4.9 Hz, $C\alpha H_{(pro\text{-}R)}$-3), 2.50 (dd, 1 H, J=12.8, 6.5 Hz, $C\alpha H_{(pro\text{-}S)}$-1), 2.27 (dd, 1 H, J=13.3, 3.5 Hz, $C\alpha H_{(pro\text{-}S)}$-7), 2.2 (dd, 1 H, J=12.8, 5.6 Hz, $C\alpha H_{(pro\text{-}S)}$-3), 1.50 (d, 3 H, J=7.5 Hz, Me), 1.48 (s, 6 H, Me), 1.43 (s, 9 H, Boc), 1.41 (d, 3 H, J=7.6 Hz, Me), 1.38 (s, 3 H, Me), 1.38 (d, 3 H, J=7.5 Hz, Me), 1.36 (d, 3 H, J=7.0 Hz, Me), 1.31 (s, 6 H, 2×Me), 1.29 (d, 3 H, J=7.6 Hz, Me), 1.28 ppm (s, 3 H, Me); ^{1}H NMR (CD_3OH, 600 MHz): δ=9.15 (d, 1 H, J=8.3 Hz, NH-3), 8.82 (d, 1 H, J=8.2 Hz, NH-5), 8.54 (d, 1 H, J=6.5 Hz, NH-8), 8.38 (d, 1 H, J=3.8 Hz, NH-2), 8.33 (d, 1 H, J=2.6 Hz, NH-4), 8.19 (d, 1 H, J=8.5 Hz, NH-6), 7.86 (d, 1 H, J=4.0 Hz, NH-7), 6.79 (d, 1 H, J=9.8 Hz, NH-1), 5.83 (d, 1 H, J=3.6 Hz, C_1H-7), 5.81 (d, 1 H, J=3.6 Hz, C_1H-1), 5.81 (d, 1 H, J=3.6 Hz, C_1H-3), 4.70 (d, 1 H, J=3.6 Hz, C_2H-1), 4.70 (d, 1 H, J=3.6 Hz, C_2H-3), 4.70 (d, 1 H, J=3.6 Hz, C_2H-7), 4.36 (qd, 1 H, J=6.5, 7.4 Hz, C_{α}H-8), 4.35 (dddd, 1 H, J=8.5, 5.1, 4.8, 9.3 Hz, C_{β}H-7), 4.34 (qd, 1 H, J=8.2, 7.0 Hz, C_{α}H-5), 4.31 (dd, 1 H, J=3.2, 9.3 Hz, C_4H-7), 4.27 (dd, 1 H, J=3.0, 7.0 Hz, C_4H-1), 4.26 (dddd, 1 H, J=8.3, 4.1, 5.9, 10.4 Hz, C_{β}H-3), 4.16 (qd, 1 H, J=3.8, 7.0 Hz, C_{α}H-2), 4.16 (dddd, 1 H, J=9.0, 3.4, 6.5, 7.0 Hz, C_{β}H-1), 4.16 (qd, 1 H, J=4.0, 6.7 Hz, C_{α}H-6), 4.10 (qd, 1 H, J=2.6, 7.0 Hz, C_{α}H-4), 4.10 (dd, 1 H, J=3.3, 10.4 Hz, C_4H-3), 3.90 (d, 1 H, J=3.3 Hz, C_3H-3), 3.85 (d, 1 H, J=3.2 Hz, C_3H-7), 3.73 (d, 1 H, J=3.2 Hz, C_3H-1), 3.70 (s, 3 H, COOMe), 3.39 (s, 3 H, OMe), 3.38 (s, 3 H, OMe), 3.38 (s, 3 H, OMe), 2.63 (dd, 1 H, J=4.1, 13.5 Hz, C_{α}H-2), 2.57 (dd, 1 H, J=5.1, 14.0 Hz, C_{α}H-7), 2.40 (dd, 1 H, J=3.4, 14.0 Hz, C_{α}H-1), 2.34 (dd, J=6.6, 14.0 Hz, C_{α}H-1), 2.33 (dd, J=4.8, 14.0 Hz, C_{α}H-7), 2.13 (dd, J=5.9, 13.5 Hz, C_{α}H-4), 1.48 (d, 1 H, J=6.7 Hz, Me), 1.43 (s, 9 H, 3×Me), 1.41 (s, 9 H, Boc), 1.39 (d, 1 H, J=7.4 Hz, Me-8), 1.34 (d, 1 H, J=7.0 Hz, Me-5), 1.34 (d, 1 H, J=7.0 Hz, Me-4), 1.34 (d, 1 H, J=7.0 Hz, Me-2), 1.28 (s, 3 H, Me), 1.28 (s, 3 H, Me), 1.27 ppm (s, 3 H, Me); ^{1}H NMR (CD_2Cl_2, 600 MHz): δ=7.91 (d, 1 H, J=7.6 Hz, NH-8), 7.85 (d, 1 H, J=9.9 Hz, NH-3), 7.79 (m, 1 H, NH-6), 7.51 (d, 1 H, J=9.7 Hz, NH-7), 7.48 (m, 1 H, NH-4), 7.38 (d, 1 H, J=9.5 Hz, NH-5), 6.66 (m, 1 H, NH-2), 5.79 (d, 1 H, J=3.8 Hz, C_1H-1), 5.76 (d, 1 H, J=3.6 Hz, C_1H-7), 5.74 (d, 1 H, J=3.6 Hz, C_1H-3), 5.58 (d, 1 H, J=8.6 Hz, NH-3), 4.53 (d, 1 H, J=3.6 Hz, C_2H-1), 4.52 (m, 2 H, C_2H-3,7), 4.42 (q, 1 H, J=7.6 Hz, C_{α}H-8), 4.33 (m, 4 H, C_{α}H-2, C_{β}H-7, C_{β}H-3, C_{α}H-5), 4.18 (m, 1 H, C_{α}H-4), 4.12 (m, 1 H, C_4H-1), 4.09 (m, 1 H, C_{β}H-1), 4.02 (m, 1 H, C_4H-7), 3.98 (m, 1 H, C_4H-3), 3.94 (m, 1 H, C_{α}H-6), 3.87 (d, 1 H, J=3.0 Hz, C_3H-7), 3.67 (d, 1 H, J=3.2 Hz, C_3H-3), 3.64 (d, 1 H, J=2.6 Hz, C_3H-1), 3.63 (s, 3 H, COOMe), 3.32 (s, 3 H, OMe), 3.31 (s, 3 H, OMe), 3.29 (s, 3 H, OMe), 2.48 (m, 3 H, C_{α}H-1, C_{α}H-7, C_{α}H-3), 2.37 (dd, 1 H, J=6.5, 14.0 Hz, C_{α}H-1), 2.16 (dd, 1 H, J=4.1, 13.2 Hz, C_{α}H-7), 2.12 (m, C_{α}H-3), 1.36 (m, 18 H, Boc, 3×Me), 1.32 (d, 3 H, Me-8), 1.29 (s, 3 H, Me), 1.26 (d, 3 H, J=7.0 Hz, Me-2), 1.24 (d, 3 H, J=7.0 Hz, Me-4), 1.22 (s, 6 H, 2×Me), 1.19 (s, 3 H, Me), 1.18 ppm (d, 3 H, J=7.3 Hz, Me-5); ^{13}C NMR (CD_3OH, 150 MHz): δ=174.52, 174.26, 173.81, 173.55, 173.13, 171.48, 171.40, 156.37, 111.49, 111.42, 111.29, 104.86, 104.79, 104.69, 83.63, 83.58, 83.40, 81.23, 81.17, 81.11, 80.93, 79.82, 79.40, 78.76, 56.30, 51.58, 50.71, 50.26, 50.18, 48.65, 48.56, 46.57, 37.34, 37.24, 37.12, 29.33, 27.43, 25.67, 25.09, 25.01, 16.49, 16.34, 16.16, 15.93, 15.70 ppm; HRMS (ESI+): m/z calcd for $C_{54}H_{88}N_8O_{23}$ [M^++Na]: 1239.5843; found: 1239.5854.

Boc-L-Ala-D-Ala-L-Ala-(*S*)-β-Caa-L-Ala-OMe (10)

A solution of acid **9** (0.15 g, 0.58 mmol), HOBt (0.1 g, 0.7 mmol), and EDCI (0.13 g, 0.70 mmol) in dry CH_2Cl_2 (10 mL) was stirred at 0 °C for 15 min and treated with salt **8** (0.06 g, 0.11 mmol) and DIPEA (0.15 mL, 0.88 mmol) under a nitrogen atmosphere for 5 h. Workup as described for **6** and purification of the residue by column chromatography (60–120 mesh silica gel, 2.8% MeOH in $CHCl_3$) afforded **10** (0.14 g, 48%) as a white solid. M.p. 164–166 °C; $[\alpha]_D^{20}$=+163.66 (c=0.1 in $CHCl_3$); IR (KBr): ν=3303, 3080, 2983, 2937, 17501, 1647, 1547, 1453, 1376, 1333, 1252, 1218, 1166, 1113, 1074, 1025, 894, 855, 761, 647, 518, 434 cm^{-1}; ^{1}H NMR ($CDCl_3$, 600 MHz): δ=7.97 (d, 1 H, J=7.6 Hz, NH-5), 7.49 (d, 1 H, J=9.5 Hz, NH-4), 7.46 (d, 1 H, J=8.4 Hz, NH-2), 7.39 (d, 1 H, J=4.4 Hz, NH-3), 5.89 (d, 1 H, J=3.7 Hz, C_1H-1), 5.24 (d, 1 H, J=6.0 Hz, NH-1), 4.61 (d, 1 H, J=3.7 Hz, C_{α} H-1), 4.56 (m, 1 H, C_{α} H-2), 4.54 (qt, 1 H, J=7.6 Hz, C_{α}H-5), 4.45 (tdd, 1 H, J=9.5, 4.7, 3.8 Hz, C_{β} H-4), 4.2 (dd, 1 H, J=3.1, 9.1 Hz, C_4H-4), 4.07 (dq, 1 H, J=4.4, 7.2 Hz, C_{α}H-3), 4.03 (qd, 1 H, J=6.0, 7.3 Hz, C_{α}H-1), 3.99 (d, 1 H, J=3.1 Hz, C_3H-4), 3.72 (s, 3 H, COOMe), 3.39 (s, 3 H, OMe), 2.58 (dd, 1 H, J=4.7, 13.5 Hz, C_{α}H-4), 2.28 (dd, 1 H, J=3.8, 13.5 Hz, $C\alpha H_{(pro\text{-}R)}$-1), 1.48 (s, 3 H, Me), 1.43 (s, 9 H, Boc and 6 H, 2×Me), 1.35 (d, 3 H, J=7.5 Hz, Me), 1.34 (d, 6 H, J=7.3 Hz, 2×Me), 1.31 ppm (s, 3 H, Me); ^{13}C NMR ($CDCl_3$, 150 MHz): δ=175.41, 173.35, 173.17, 172.66, 170.77, 155.79, 111.66, 104.85, 83.24, 81.20, 80.22, 79.80, 57.35, 52.61, 51.01, 50.75, 48.55, 47.96, 46.57, 38.12, 28.23, 26.66, 26.32, 17.52, 17.16, 16.82, 16.22 ppm;

HRMS (ESI+): m/z calcd for $C_{29}H_{49}N_5O_{12}$ $[M^+ +H]$: 660.347; found: 660.345.

Boc-(S)-β-Caa-L-Ala-(S)-β-Caa-L-Ala-D-Ala-L-Ala-D-Ala-L-Ala-(S)-β-Caa-L-Ala-OMe (3)

A solution of ester **6** (0.19 g, 0.22 mmol) treated as described above gave **6a** (0.16 g, 86%) as a white solid, which was used for the next reaction without further purification.

A solution of **6a** (0.14 g, 0.17 mmol), HOBt (0.03 g, 0.19 mmol), and EDCI (0.04 g, 0.19 mmol) in dry CH_2Cl_2 (10 mL) was stirred at 0°C for 15 min and treated with salt **10 a** [prepared from **10** (0.12 g, 0.17 mmol) and CF_3COOH (0.1 mL) in dry CH_2Cl_2 (0.9 mL) at 0°C] and DIPEA (0.04 mL, 0.24 mmol) under a nitrogen atmosphere for 5 h. Workup as described for **6** and purification of the residue by column chromatography (60–120 mesh silica gel, 5.2% MeOH in $CHCl_3$) afforded **7** (0.08 g, 35%) as a white solid. M.p. 243–245°C; $[\alpha]_D^{20}=+27.08$ ($c=0.1$ in $CHCl_3$); IR ($CHCl_3$): $\nu=3422$, 3318, 2961, 2931, 2875, 2854, 1728, 1661, 1534, 1455, 1378, 1296, 1255, 1164, 1119, 1081, 1021, 888, 856, 750 cm^{-1}; ^1H NMR ($CDCl_3$, 600 MHz): $\delta=$ 8.15 (d, 1H, $J=6.5$ Hz, NH-5), 7.92 (d, 1H, $J=6.8$ Hz, NH-1), 7.86 (d, 1H, $J=6.7$ Hz, NH-6), 7.78 (d, 1H, $J=4.1$ Hz, NH-4), 7.74 (d, 1H, $J=6.7$ Hz, NH-3), 7.67 (d, 1H, $J=4.0$ Hz, NH-8), 7.43 (d, 1H, $J=5.4$ Hz, NH-7), 7.54 (d, 1H, $J=8.4$ Hz, NH-9), 6.77 (d, 1H, $J=4.0$ Hz, NH-2), 5.92 (d, 1H, $J=3.6$ Hz, C_1H-1), 5.91 (d, 1H, $J=3.6$ Hz, C_1H-3), 5.87 (d, 1H, $J=3.6$ Hz, C_1H-9), 5.65 (d, 1H, $J=7.8$ Hz, NH-1), 4.59 (d, 1H, $J=3.6$ Hz, C_2H-3), 4.59 (d, 1H, $J=3.6$ Hz, C_2H-9), 4.58 (d, 1H, $J=3.6$ Hz, C_2H-1), 4.55 (dq, 1H, $J=6.8$, 6.0 Hz, C_αH-1), 4.47 (dd, 1H, $J=9.6$, 6.7, 5.6 Hz, C_βH-3), 4.47 (dq, 1H, $J=6.0$, 6.7 Hz, C_αH-6), 4.43 (dd, 1H, $J=8.4$, 9.6 Hz, C_βH-9), 4.42 (dq, $J=5.4$, 6.6 Hz, C_αH-7), 4.38 (dq, 1H, $J=6.5$, 7.5 Hz, C_αH-5), 4.34 (dq, 1H, $J=4.1$, 6.5 Hz, C_αH-4), 4.34 (dd, 1H, $J=9.6$, 3.2 Hz, C_4H-3), 4.30 (m, 1H, C_4H-1), 4.22 (dq, 1H, $J=4.0$, 7.1 Hz, C_αH-2), 4.19 (dd, 1H, $J=9.6$, 3.2 Hz, C_αH-9), 4.05 (dq, 1H, $J=4.0$, 7.1 Hz, C_αH-8), 4.00 (d, 1H, $J=3.2$ Hz, C_3H-9), 3.90 (d, 1H, $J=3.2$ Hz, C_3H-3), 3.74 (d, 1H, $J=3.3$ Hz, C_3H-1), 3.72 (s, 3H, COOMe), 3.40 (s, 3H, OMe), 3.38 (s, 3H, OMe), 3.37 (s, 3H, OMe), 2.65 (dd, 1H, $J=14$, 4.9 Hz, $C\alpha H_{(pro\text{-}R)}$-3), 2.58 (dd, 1H, $J=13.2$, 4.5 Hz, $C\alpha H_{(pro\text{-}R)}$-9), 2.53 (dd, 1H, $J=14.0$, 4.3 Hz, $C\alpha H_{(pro\text{-}R)}$-1), 2.42 (dd, 1H, $J=14.0$, 6.0 Hz, $C\alpha H_{(pro\text{-}S)}$-1), 2.26 (dd, 1H, $J=13.2$, 5.6 Hz, $C\alpha H_{(pro\text{-}R)}$-9), 2.24 (dd, 1H, $J=14.0$, 5.6 Hz, $C\alpha H_{(pro\text{-}S)}$-3), 1.49 (s, 3H, Me), 1.47 (s, 3H, Me), 1.45 (s, 3H, Me), 1.45 (d, 3H, $J=7.0$ Hz, Me), 1.43 (d, 3H, $J=6.5$ Hz, Me), 1.43 (s, 9H, Boc), 1.38 (d, 3H, $J=7.1$ Hz, Me), 1.38 (d, 3H, $J=7.1$ Hz, Me), 1.34 (d, 3H, $J=7.5$ Hz, Me), 1.32 (s, 3H, Me), 1.31 (s, 6H, Me), 1.29 ppm (d, 3H, $J=6.6$ Hz, Me); ^1H NMR (CD_3OH, 600 MHz): $\delta=8.94$ (d, 1H, $J=8.5$ Hz, NH-3), 8.70 (d, 1H, $J=7.8$ Hz, NH-5), 8.53 (d, 1H, $J=7.4$ Hz, NH-7), 8.48 (d, 1H, $J=6.8$ Hz, NH-10), 8.34 (d, 1H, $J=3.4$ Hz, NH-4), 8.33 (d, 1H, $J=4.4$ Hz, NH-2), 8.08 (d, 1H, $J=8.9$ Hz, NH-9), 8.04 (d, 1H, $J=4.4$ Hz, NH-6), 8.01 (d, 1H, $J=5.9$ Hz, NH-8), 6.74 (d, 1H, $J=9.1$ Hz, NH-1), 5.85 (d, 1H, $J=3.6$ Hz, C_1H-9), 5.84 (d, 1H, $J=3.6$ Hz, C_1H-3), 5.82 (d, 1H, $J=3.6$ Hz, C_1H-1), 4.70 (d, 1H, $J=3.6$ Hz, C_2H-1), 4.70 (d, 1H, $J=3.6$ Hz, C_2H-3), 4.70 (d, 1H, $J=3.6$ Hz, C_2H-9), 4.38 (dddd, 1H, $J=8.0$, 4.9, 3.5, 9.6 Hz, C_βH-9), 4.36 (dd, 1H, $J=7.8$, 7.0 Hz, C_αH-5), 4.36 (dd, 1H, $J=6.8$, 7.2 Hz, C_αH-10), 4.31 (dddd, 1H, $J=4.3$, 4.9, 8.5, 9.6 Hz, C_βH-3), 4.27 (d, 1H, $J=7.4$ Hz, C_αH-7), 4.26 (dd, $J=3.5$, 9.6 Hz, C_4H-9), 4.21 (dq, 1H, $J=4.0$, 7.2 Hz, C_αH-8), 4.19 (m, 1H, C_β-1), 4.18 (dd, 1H, $J=4.4$, 7.2 Hz, C_αH-6), 4.16 (dq, 1H, $J=3.4$, 6.5 Hz, C_αH-4), 4.16 (m, 1H, C_4H-1), 4.15 (dq, 1H, $J=4.4$, 7.0 Hz, C_αH-2), 4.15 (dd, 1H, $J=3.0$, 9.6 Hz, C_4H-3), 3.63 (s, 3H, COOMe), 3.31 (s, 3H, OMe), 3.31 (s, 3H, OMe), 3.30 (s, 3H, OMe), 3.88 (d, 1H, $J=3.0$ Hz, C_3H-3), 3.80 (d, 1H, $J=3.5$ Hz, C_3H-9), 3.73 (d, 1H, $J=3.0$ Hz, C_3H-1), 2.60 (dd, 1H, $J=4.3$, 13.7 Hz, C_αH-3), 2.51 (dd, 1H, $J=4.9$, 14.0 Hz, C_αH- 9), 2.40 (dd, 1H, $J=5.6$, 14.0 Hz, C_αH-1), 2.40 (dd, 1H, $J=3.5$, 14.0 Hz, C_αH-9), 2.36 (dd, 1H, $J=7.4$, 14.0 Hz, C_αH-1), 2.18 (dd, 1H, $J=4.9$, 13.7 Hz, C_αH-3), 1.46 (d, 3H, $J=7.2$ Hz, Me-6), 1.38 (d, 3H, $J=7.2$ Hz, Me-8), 1.38 (d, 3H, $J=7.2$ Hz, Me-10), 1.36 (d, 3H, $J=7.0$ Hz, Me-2), 1.36 (d, 3H, $J=7.4$ Hz, Me-7), 1.36 (s, 3H, Me), 1.35 (s, 6H, 2×Me), 1.34 (d, 3H, $J=6.5$ Hz, Me-4), 1.34 (d, 3H, $J=7.0$ Hz, Me-5), 1.33 (s, 9H, 3×Me, Boc), 1.27 ppm (s, 9H, 3×Me); ^{13}C NMR (CD_3OH, 175 MHz): $\delta=174.58$, 174.19, 174.06, 173.91, 173.55, 173.29, 173.21, 171.44, 171.37, 171.31, 156.37, 111.47, 111.39, 111.22, 104.86, 104.79, 104.68, 83.87 (3C), 83.41, 81.15, 81.15, 81.10, 81.01, 80.92, 79.81, 79.28, 79.69, 56.25 (2C), 56.45, 51.55, 50.61, 50.24, 49.90, 49.25, 46.64, 46.54, 37.28, 37.21, 37.13, 27.41 (3C), 25.68, 25.63, 25.53, 25.09, 25.03, 25.99, 16.39, 16.17, 16.06 (2C), 15.82, 15.74 ppm; HRMS (ESI+): m/z calcd for $C_{60}H_{98}N_{10}O_{25}$ $[M^+ +Na]$: 1381.66011; found: 1381.65968.

Acknowledgements

P.P.R. and G.V. are thankful to CSIR, New Delhi, India, for financial support in the form of research fellowships. All of the authors thank CSIR, New Delhi, India, for financial support as research grants.

Keywords: chirality · helical induction · helical structures · hybrid structures · peptides

[1] D. J. Hill, M. J. Mio, R. B. Prince, T. S. Hughes, J. S. Moore, *Chem. Rev.* **2001**, *101*, 3893–4011.
[2] a) D. Seebach, M. Overhand, F. N. M. Kuhnle, B. Martinoni, L. Oberer, U. Hommel, H. Widmer, *Helv. Chim. Acta* **1996**, *79*, 913–941; b) D. H. Appella, L. A. Christianson, I. L. Karle, D. R. Powell, S. H. Gellman, *J. Am. Chem. Soc.* **1996**, *118*, 13071–13072.
[3] S. H. Gellman, *Acc. Chem. Res.* **1998**, *31*, 173–180.
[4] a) D. Seebach, K. Gademann, J. V. Schreiber, J. L. Matthews, T. Hintermann, B. Jaun, L. Oberer, U. Hommel, H. Widmer, *Helv. Chim. Acta* **1997**, *80*, 2033–2038; b) K. Möhle, R. Günther, M. Thormann, N. Sewald, H.-J. Hofmann, *Biopolymers* **1999**, *50*, 167–184; c) S. A. W. Gruner, V. Truffault, G. Voll, E. Locardi, M. Stockle, H. Kessler, *Chem. Eur. J.* **2002**, *8*, 4365–4376; d) P. I. Arvidsson, N. S. Ryder, H. M. Weiss, G. Gross, O. Kretz, R. Woessner, D. Seebach, *ChemBioChem* **2003**, *4*, 1345–1347; e) Y.-D. Wu, W. Han, D.-P. Wang, Y. Gao, Y. L. Zhao, *Acc. Chem. Res.* **2008**, *41*, 1418–1427.
[5] a) D. Seebach, A. K. Beck, D. Birbaum, *J. Chem. Biodiversity* **2004**, *1*, 1111–1239; b) S. Hecht, I. Huc, *Foldamers: Structure, Properties and Applications*, Wiley-VCH, Weinheim, **2007**; c) T. A. Martinek, F. Fülöp, *Chem. Soc. Rev.* **2012**, *41*, 687–702.
[6] a) A. Hayen, M. A. Schmitt, N. Nagassa, K. A. Thomson, S. H. Gellman, *Angew. Chem.* **2004**, *116*, 511–516; *Angew. Chem. Int. Ed.* **2004**, *43*, 505–510; b) S. De Pol, C. Zorn, C. D. Klein, O. Zerbe, O. Reiser, *Angew. Chem.* **2004**, *116*, 517–520; *Angew. Chem. Int. Ed.* **2004**, *43*, 511–514; c) D. Seebach, B. Jaun, R. Sebesta, R. I. Mathad, O. Flogel, M. Limbach, H. Sllner, S. Cottens, *Helv. Chim. Acta* **2006**, *89*, 1801–1825; d) B. Jagadeesh, A. Prabhakar, G. D. Sarma, S. Chandrasekhar, G. Chandrashekar, M. S. Reddy, B. Jagannadh, *Chem. Commun.* **2007**, 371–373; e) W. S. Horne, S. H. Gellman, *Acc. Chem. Res.* **2008**, *41*, 1399–1408; f) L. K. A. Pilsl, O. Reiser, *Amino Acids* **2011**, *41*, 709–718; g) G. V. M. Sharma, T. A. Yadav, C. Madhavi, A. C. Kunwar, *J. Org. Chem.* **2012**, *77*, 6834–6848; h) D. Balamurugan, K. M. Muraleedharan, *Chem. Eur. J.* **2012**, *18*, 9516–9520.
[7] a) G. V. M. Sharma, P. Nagendar, P. Jayaprakash, P. R. Krishna, K. V. S. Ramakrishna, A. C. Kunwar, *Angew. Chem.* **2005**, *117*, 6028–6032; *Angew. Chem. Int. Ed.* **2005**, *44*, 5878–5882; b) C. Baldauf, R. Günther, H. J. Hofmann, *Biopolymers* **2006**, *84*, 408–413; c) G. V. M. Sharma, G. Srinivasulu, S. Kiran Kumar, A. C. Kunwar, *J. Org. Chem.* **2006**, *71*, 8395–8400; d) G. V. M. Sharma, P. Nagendar, K. V. S. Ramakrishna, N. Chandramouli, M. Choudhary, A. C. Kunwar, *Chem. Asian J.* **2008**, *3*, 969–983;

e) G. V. M. Sharma, K. S. Reddy, S. J. Basha, K. R. Reddy, A. V. S. Sarma, *Org. Biomol. Chem.* **2011**, *9*, 8102 – 8111.
[8] a) G. V. M. Sharma, V. B. Jadhav, K. V. S. Ramakrishna, P. Jayaprakash, K. Narsimulu, V. Subash, A. C. Kunwar, *J. Am. Chem. Soc.* **2006**, *128*, 14657 – 14668; b) C. Baldauf, R. Günther, H. J. Hofmann, *J. Org. Chem.* **2006**, *71*, 1200 – 1208; c) G. V. M. Sharma, V. Manohar, S. K. Dutta, V. Subash, A. C. Kunwar, *J. Org. Chem.* **2008**, *73*, 3689 – 3698; d) G. V. M. Sharma, B. S. Babu, D. Chatterjee, K. V. S. Ramakrishna, A. C. Kunwar, P. Schramm, H. J. Hofmann, *J. Org. Chem.* **2009**, *74*, 6703 – 6713; e) G. V. M. Sharma, A. C. Kunwar, in *Recent Research Developments in Foldamer Chemistry* (Ed.: Y. V. D. Nageswar), Nova Science Publishers Inc., New York **2012**.
[9] L. Berlicki, L. Pilsl, E. Weber, I. M. Mandity, C. Cabrele, T. A. Martinek, F. Fulop, O. Reiser, *Angew. Chem.* **2012**, *124*, 2251 – 2255; *Angew. Chem. Int. Ed.* **2012**, *51*, 2208 – 2212.
[10] A. S. Arseniev, I. L. Barsukov, V. F. Bystrove, A. L. Lomize, Y. A. Ovichinikove, *FEBS Lett.* **1985**, *186*, 168 – 174.
[11] E. Navarro, R. Tejero, E. Fenude, B. Celda, *Biopolymers* **2001**, *59*, 110 – 119.
[12] J. C. Dean, E. G. Buchanan, T. S. Zwier, *J. Am. Chem. Soc.* **2012**, *134*, 17186 – 17201.
[13] C. Baldauf, R. Gunther, H. J. Hofmann, *Angew. Chem.* **2004**, *116*, 1621 – 1624; *Angew. Chem. Int. Ed.* **2004**, *43*, 1594 – 1597.
[14] S. G. Itoh, H. J. Okumura, *J. Phys. Soc. Jpn.* **2011**, *80*, 094801.
[15] J. D. Sadowsky, M. A. Schmitt, H. S. Lee, N. Umezawa, S. Wang, Y. Tomita, S. H. Gellman, *J. Am. Chem. Soc.* **2005**, *127*, 11966 – 11968.
[16] G. V. M. Sharma, N. Chandramouli, M. Choudhary, P. Nagendar, K. V. S. Ramakrishna, A. C. Kunwar, P. Schramm, H. J. Hofmann, *J. Am. Chem. Soc.* **2009**, *131*, 17335 – 17344.
[17] G. V. M. Sharma, K. S. Reddy, S. K. Dutta, V. Subash, K. Narsimulu, G. Anjaiah, S. J. Basha, A. C. Kunwar, *Chem. Eur. J.* **2012**, *18*, 16046 – 16060.
[18] a) G. V. M. Sharma, K. R. Reddy, P. R. Krishna, A. R. Sankar, K. Narsimulu, S. K. Kumar, P. Jayaprakash, B. Jagannadh, A. C. Kunwar, *J. Am. Chem. Soc.* **2003**, *125*, 13670 – 13671; b) G. V. M. Sharma, K. R. Reddy, P. R. Krishna, A. R. Sankar, K. Narsimulu, S. K. Kumar, P. Jayaprakash, B. Jagannadh, A. C. Kunwar, *Angew. Chem.* **2004**, *116*, 4051 – 4055; *Angew. Chem. Int. Ed.* **2004**, *43*, 3961 – 3965.
[19] B. Forood, E. J. Feliciano, K. P. Nambiar, *Proc. Natl. Acad. Sci. USA* **1993**, *90*, 838 – 842.
[20] a) L. C. Chan, G. B. Cox, *J. Org. Chem.* **2007**, *72*, 8863 – 8869; b) M. Bodanszky, *Peptide Chemistry: A Practical Textbook*, Springer, New York, **1988**.
[21] See the Supporting Information.
[22] In the solvent titration studies, up to 33% (v/v) of [D$_6$]DMSO was sequentially added to $CDCl_3$ solutions of the peptides (600 μL).
[23] M. Lee, J. Shim, P. Kang, I. A. Guzei, S. H. Choi, *Angew. Chem.* **2013**, *125*, 12796 – 12799; *Angew. Chem. Int. Ed.* **2013**, *52*, 12564 – 12567.
[24] A. K. Bolin, G. L. Millhauser, *Acc. Chem. Res.* **1999**, *32*, 1027 – 1033.
[25] P. D. Thomas, V. J. Basus, T. L. James, *Proc. Natl. Acad. Sci. USA* **1991**, *88*, 1237 – 1241.

Received: April 19, 2014
Published online on July 23, 2014

